Icosahedral medium-range order formed in $Mg_{70}Zn_{30}$ metallic glass: a larger-scale molecular dynamics simulation*

Hou Zhao-Yang(侯兆阳)[a)†], Liu Rang-Su(刘让苏)[b)], Tian Ze-An(田泽安)[b)], and Wang Jin-Guo(王晋国)[a)]

[a)] *College of Science, Xidian University, Xi'an* 710071, *China*

[b)] *School of Physics and Microelectronics Science, Hunan University, Changsha* 410082, *China*

(Received 5 November 2010; revised manuscript received 8 January 2011)

A larger-scale $Mg_{70}Zn_{30}$ alloy system including 100000 atoms has been simulated by using the molecular dynamics method to investigate the icosahedral medium-range order (IMRO) formed in the $Mg_{70}Zn_{30}$ metallic glass. It is found that the simulated pair distribution function of $Mg_{70}Zn_{30}$ metallic glass is in good agreement with the experimental results. The glass transition temperature T_g is near 450 K under the cooling rate of 1×10^{12} K/s. The icosahedral local structures play a critical role in the formation of metallic glass, and they are the dominant local configurations in the $Mg_{70}Zn_{30}$ metallic glass. The IMRO in the $Mg_{70}Zn_{30}$ metallic glass is characterized by certain types of extended icosahedral clusters combined by intercross-sharing atoms in the form of chains or dendrites. The size distributions of these IMRO clusters present a magic number sequence of 19, 23, 25, 27, 29, 31, 33, 35, 37, 39,. . . , and the magic clusters can be classified into three types according to their compactness. The IMRO clusters grow rapidly in a low-dimensional way with cooling, but this growth is limited near T_g.

Keywords: molecular dynamics simulation, medium-range order, $Mg_{70}Zn_{30}$ metallic glass

PACS: 61.20.Ne, 64.70.pe, 81.70.pe, 61.46.Bc **DOI:** 10.1088/1674-1056/20/6/066102

1. Introduction

Since local atomic structures play a crucial role in understanding the glass-forming mechanism and unique properties, characterizations of the local atomic structures, in particular the short-range order (SRO) and medium-range order (MRO) structures, have been subjected to many interests.[1,2] Metallic glasses being stable at room temperature are usually composed of several elements and at least one of which is a transition metal, but the Mg–Zn alloy is one of a few glass alloys containing only two simple metallic elements.[3] Its phase diagram shows a deep eutectic at the composition $Mg_{70}Zn_{30}$, which facilitates the glass formation,[4] thus the $Mg_{70}Zn_{30}$ alloy is very attractive for experimental and theoretical studies of fundamental physical properties of metallic glasses.[5−10]

Ordered regions in the $Mg_{70}Zn_{30}$ metallic glass were observed by the X-ray and neutron diffraction experiments.[5,6] It was even addressed that the local atomic structures in the $Mg_{70}Zn_{30}$ metallic glass were rather closely related to the crystalline one which has been described as an arrangement of icosahedra,[7] and the icosahedral SRO (ISRO) has long been believed as the essential ingredient of many metallic glasses.[11−13] But a comprehensive understanding of the icosahedral MRO (IMRO) formed in the $Mg_{70}Zn_{30}$ metallic glass is still lacking because most experimental evidence is still limited to the pair distribution function (PDF), structure factor and coordination number (CN). These structural characterization methods make it difficult to reveal the detailed atomic packing of the MRO in metallic glasses. Molecular dynamics (MD) simulations provide a powerful method to study the atomic structural features of metallic glasses and monitor their formation processes during the liquid quenching processes. Recently, several packing schemes of solute-centred clusters, such as the efficient cluster packing on an fcc lattice[14] and the icosahedral packing[15] as in a quasi-crystal, have been proposed, which provides first insights on the MRO in metallic glasses. However, as the limitation of computing

*Project supported by the National Natural Science Foundation of China (Grant No. 50831003) and the Special Fund for Basic Scientific Research of Central Colleges, Chang'an Univeristy (Grant No. CHD2009JC169).

†Corresponding author. E-mail: zhaoyanghou@163.com

© 2011 Chinese Physical Society and IOP Publishing Ltd

power most simulations are restricted in a small-scale system with 500∼1000 atoms. In this small system, it is unreliable to study the MRO structures which include several hundreds of atoms.

Accordingly, in this paper, a larger-scale $Mg_{70}Zn_{30}$ system consisting of 100000 atoms is simulated by using the MD method. The formation and structure of the IMRO in the $Mg_{70}Zn_{30}$ simple metallic glass are investigated in detail by means of the PDF, Honeycutt–Anderson (HA) bond-type index method[16] and cluster-type index method (CTIM).[17−19]

2. Simulation methods

The MD simulations are performed for a larger-scale system containing 100000 atoms (i.e. 70000 Mg atoms and 30000 Zn atoms) in a cubic box with the periodic boundary conditions under constant pressure. The interatomic potentials of Mg–Zn alloy used in this paper are the effective pair potentials derived from the generalized non-local model pseudopotential (GNMP) based upon the first-principle interaction force in the second order perturbation theory,[20,21] and the function is

$$V_{ij}(r) = \frac{Z_{\mathrm{eff},i}Z_{\mathrm{eff},j}}{r}\left\{1-\left(\frac{1}{\pi}\right)\times\int_o^\infty \mathrm{d}q[F_{i,j}(q)+F_{j,i}(q)]\frac{\sin(rq)}{q}\right\}, \quad (1)$$

where Z_{eff} and $F(q)$ are, respectively, the effective ionic valence and the normalized energy wave number characteristic, which are defined in detail in Refs. [20] and [21]. For the simple metals and their alloys, the accuracy and reliability of the effective pair potentials derived from the GNMP have been demonstrated extensively by calculating their structural, dynamic and thermodynamic properties.[22,23] The pair potentials are cut off at 20 a.u. (atomic unit). The motion equations are integrated by using the leap-frog algorithm with a time step of 5 fs.

The simulation calculations start at 1173 K (the melting point T_{m} of $Mg_{70}Zn_{30}$ alloy is near 616 K). First of all, let the system run 50000 time steps at 1173 K to obtain an equilibrium liquid state determined by the energy changes of the system. Then the damped force method[24,25] (also called the Gaussian thermostat) is adopted to decrease the system temperature to 273 K at a cooling rate of 1×10^{12} K/s. The intervals between two temperature points are 100 K. At each given temperature, the instantaneous spatial coordinates of each atom are recorded for the analyses of microstructure below. Finally, the structural analyses are performed in terms of the PDF, HA bond-type index method and CTIM.

3. Results and discussions

3.1. Comparisons with experimental results

Since the PDF is a Fourier transformation of the structure factor obtained from diffraction experiment, it can be used to compare the simulation results with the experimental ones for liquid and glass structures. Figure 1 shows the evolution of the total PDF during the rapid quenching processes of $Mg_{70}Zn_{30}$ liquid alloy. The experimental results of the PDFs at 673 K (liquid) and 293 K (glass) come from a conversion of the reduced PDF in Ref. [5] measured by the neutron diffraction. It is clearly seen that the splitting on the second peak of total PDF becomes pronounced with the decreasing temperature, which indicates the formation of $Mg_{70}Zn_{30}$ metallic glass and the enhancement of SRO during the quenching processes. The simulated total PDFs for the liquid and glass structures both agree well with the experimental results except for their slightly higher first peaks.

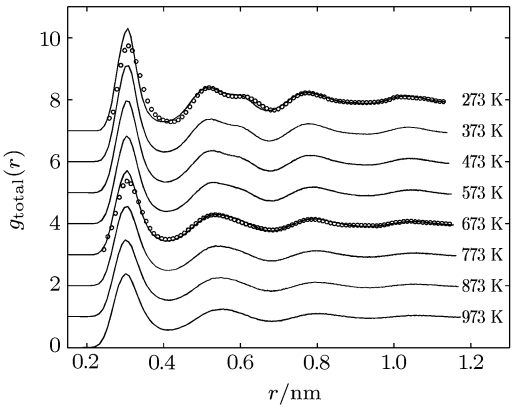


Fig. 1. Evolutions of total PDF during the liquid quenching processes of $Mg_{70}Zn_{30}$ alloy. Experimental points are taken from Ref. [5] measured by neutron diffraction.

Based on the simulated total PDF, the glass transition temperature T_{g} can be obtained by the relations of the Wendt–Abraham ratio R[26] with temperature, as shown in Fig. 2. The T_{g} is estimated to be 450 K, which is higher than that of experimental result ($\approx$ 370 K).[27] Considering the much higher cooling rate adopted in the present simulation (1×10^{12} K/s)

than that appearing in experiment will enhance the T_g, we find that our calculations are reasonable.

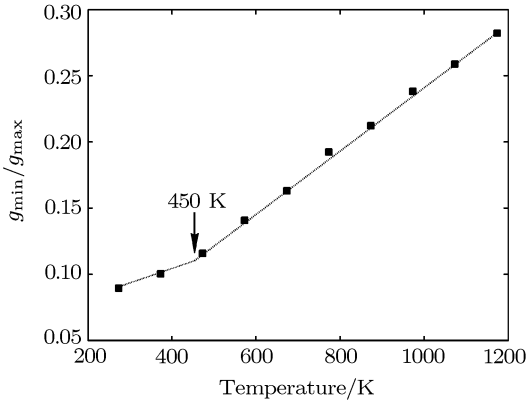


Fig. 2. Relations of Wendt–Abraham ratio $R = g_{min}/g_{max}$ with temperature obtained from Fig. 1.

3.2. ISRO

The PDF and CN reflect the SRO structures in a statistical average, but they are incapable of describing topological structures of the SRO. The HA bond-type index method[16] has been widely used to assess the local configurations of the liquid, amorphous and crystal structures. In this method, a set of four integers *ijkl* is designed to describe the different local configurations. The first integer i identifies the bonding of two given atoms. i is 1 when they are bonded in the root pair, otherwise i is 2. The second integer j is the number of common near-neighbour atoms shared by the root pair. The third integer k is the number of bonds among the shared neighbours. The fourth integer l is needed to distinguish configurations having the same first three indices but being different bond geometries. Different local atomic structures have different HA indices and general observations are as follows: the fcc crystal structure leads only to 1421 bond-type; the hcp crystal structure leads to 50% 1421 bond-type and 50% 1422 bond-type; the bcc crystal structure has 43% 1441 bond-type and 57% 1661 bond-type; while the 13-atom icosahedron has twelve 1551 bond-types. When one bond between a pair of outer atoms in an icosahedron is broken, two of the 1551 bond-types transform into 1541 bond-types and two transform into 1431 bond-types.

Figure 3 shows the evolutions of a relative number of various bond-types during the rapidly quenching processes of $Mg_{70}Zn_{30}$ alloy. It can be seen that there are some different bond-types in the system during the quenching processes, but the numbers of 1551, 1541, and 1431 bond-types closely related to the icosahedral or defective ISRO are significantly higher than the other types and their summation reaches to 74.2% in the glass structure at 273 K. Moreover, the 1551 bond-type increases remarkably during the glass transition process, whereas others change a little. This means that various SRO structures in $Mg_{70}Zn_{30}$ alloy liquid characterized by the different HA bond-type indices are inherited to the glass structure during the rapidly quenching processes and the ISRO structures play a critical role in the formation of the $Mg_{70}Zn_{30}$ metallic glass.

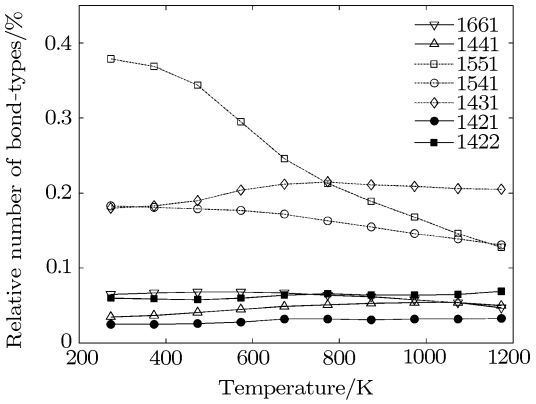


Fig. 3. Evolutions of relative numbers of various bond-types during the rapidly quenching processes of $Mg_{70}Zn_{30}$ alloy.

Just as the 1551 bond-type only reveals the presence of fragments of icosahedron, the HA bond-type index method is incapable of characterizing atomic cluster structures, especially the larger clusters with MRO. Based on the HA bond-type index, we have proposed a new method—CTIM[17−19] to describe the topological structures of different atomic clusters. We define the basic cluster as the smallest cluster composed of one central atom and its nearest-neighbour atoms and the CTIM adopts four indices (N, n_1, n_2, n_3) to denote different types of basic clusters, where N is the number of the nearest-neighbour atoms and n_1, n_2, n_3 denotes the numbers of 1441, 1551, and 1661 bond-types formed between the surrounding atoms and the central atom, respectively. For example, the (9 3 6 0) and (10 2 8 0) respectively stand for the Bernal polyhedrons of tri-capped trigonal prism and bi-capped square archimedean antiprism; the icosahedron can be expressed as (12 0 12 0); the CN14, CN15, and CN16 Frank–Kasper polyhedrons can be respectively expressed as (14 0 12 2), (15 0 12 3), and (16 0 12 4). The schematic configurations of these basic clusters are given in Fig. 4.

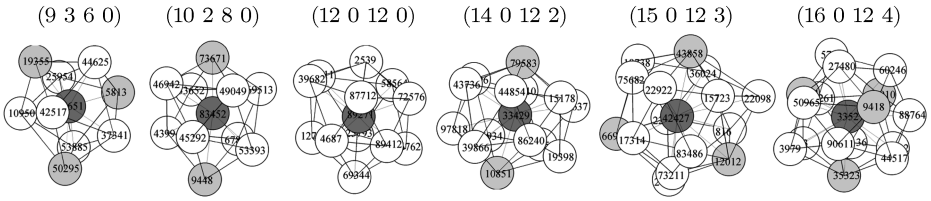


Fig. 4. Schematic configurations of six typical basic clusters with bondings and labels of atoms in $Mg_{70}Zn_{30}$ metallic glass at 273 K.

According to the CTIM, we can obtain the statistical numbers of various basic clusters in the $Mg_{70}Zn_{30}$ liquid (573 K) and glass (273 K) structures, as listed in Table 1.

Table 1. Numbers of various types of basic clusters in $Mg_{70}Zn_{30}$ liquid (573 K) and glass (273 K) structures.

Type of clusters	Numbers			
	Liquid		Glass	
	Mg	Zn	Mg	Zn
(17 0 12 5)	3	0	1	0
(17 1 10 6)	11	0	4	0
(17 2 8 7)	5	0	3	0
(17 3 6 8)	0	0	1	0
(16 0 12 4)	24	0	151	0
(16 1 10 5)	62	0	133	0
(16 2 8 6)	35	0	40	0
(16 3 6 7)	13	0	3	0
(16 4 4 8)	2	0	3	0
(15 0 12 3)	58	0	357	0
(15 1 10 4)	148	1	378	0
(15 2 8 5)	113	1	206	0
(15 3 6 6)	52	0	58	0
(15 4 4 7)	15	0	17	0
(14 0 12 2)	122	3	454	10
(14 1 10 3)	162	4	287	2
(14 2 8 4)	224	11	298	6
(14 3 6 5)	66	3	44	0
(14 4 4 6)	43	3	22	0
(13 1 10 2)	279	74	567	100
(13 2 8 3)	48	26	19	10
(13 3 6 4)	113	56	69	59
(13 4 4 5)	4	6	1	4
(13 5 2 6)	0	4	0	2
(12 0 12 0)	302	664	1115	4480
(12 2 8 2)	37	296	38	725
(12 3 6 3)	7	81	0	61
(12 4 4 4)	5	32	1	20
(11 2 8 1)	4	310	2	491
(11 3 6 2)	1	37	0	24
(11 4 4 3)	0	34	0	15
(10 2 8 0)	0	121	0	126
(10 3 6 1)	0	59	0	27
(10 4 4 2)	0	8	0	1
(9 3 6 0)	0	29	0	15
Total number	1958	1863	4267	6178

It can be clearly seen that there are many different types of basic clusters in the liquid and glass structures and these basic clusters centred by the larger Mg atoms mostly are CN14, CN15, and CN16 Frank–Kasper polyhedrons and their distorted cases which possess larger CN; while those centered by the smaller Zn atoms mostly are icosahedron, Bernal polyhedron and their distorted cases which possess smaller CN. When the alloy liquid is quenched to its glass structure, the icosahedron and Frank–Kasper polyhedrons both increase rapidly except for the Bernal polyhedrons and the increase of Zn-centred icosahedron is most significant. This is easy to understand because the distance between surface neighbour atoms is about 5% larger than that from the centre to the surface atom. The small Zn atoms located at the centres of icosahedra can release this frustration easily. In the $Mg_{70}Zn_{30}$ metallic glass, the summation of various basic clusters reaches 10445 which contain 65.03% of the total 100000 atoms in the system. The 74.71% of these basic clusters are icosahedra and their distorted cases with CN of 11, 12, and 13, while the Bernal polyhedrons of (9 3 6 0) and (10 2 8 0) are very few. This indicates that the SRO in $Mg_{70}Zn_{30}$ metallic glass can be modeled by neither the widely cited Bernal's dense random packing model[28] nor the stereochemically defined model,[29] but rather various types of basic clusters characterized by the different CTIM indices and the ISRO structure is the dominant structural units.

3.3. IMRO

When two icosahedra are linked by vertex-sharing (VS), edge-sharing (ES), face-sharing (FS) or intercross-sharing (IS) atoms, extended icosahedral clusters with IMRO can be formed. We regard the different linkages between two icosahedra as VS, ES, FS, and IS cluster bond-types. Figure 5 shows the schematic configurations of different cluster bond-types between two icosahedra and the evolutions of their numbers with temperature during the rapidly

quenching processes. From Fig. 5(b), it can be found that in the high temperature liquid above T_m, most icosahedra in system are isolated from each other and their numbers change little with the decrease of temperature. When the temperature continuously decreases from T_g, the number of isolated icosahedra begins to decrease, more and more icosahedra are linked with each other by the VS, ES, FS, and IS cluster bond-types. Among the four cluster bond-types, the IS bond-type increases remarkably and is the dominant cluster bond-type in the supercooled liquid and glass structures. This indicates that the extended icosahedral clusters in the $Mg_{70}Zn_{30}$ supercooled liquid and glass structures are mainly composed of the IS cluster bond-type. Since the central atoms of two icosahedra bond with each other by sharing four atoms in the IS cluster bond-type as shown in Fig. 5(a), it is high densely packed and will be more stable than other cluster bond-types. According to the above features of the extended icosahedral clusters in the supercooled liquid and glass structures, we simplify the description of the IMRO by adopting the extended icosahedral clusters combined by only the IS cluster bond-type.

Figure 6 shows the evolutions of the maximum IMRO clusters during the quenching processes of $Mg_{70}Zn_{30}$ alloy. From Fig. 6(a), it can be found that the size of IMRO cluster remains rather small in the high temperature liquid above T_m. It grows rapidly with cooling in the supercooled region, but this growth is limited near the T_g by frustration effects coming from the difficulty in close packing three-dimensional space. From the schematic configurations of the combination of the IS cluster bond-types in the

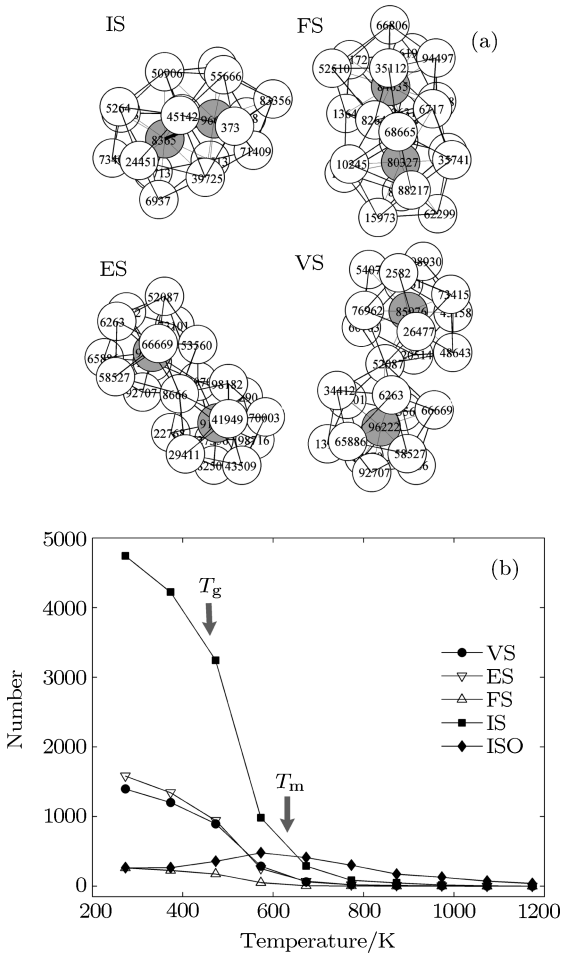


Fig. 5. (a) Schematic configurations of the VS, ES, FS, and IS cluster bond-types between two icosahedra in $Mg_{70}Zn_{30}$ metallic glass. (b) Evolutions of the numbers of VS, ES, FS, and IS bonds and the isolated icosaheron in the system with temperature during the rapidly quenching processes.

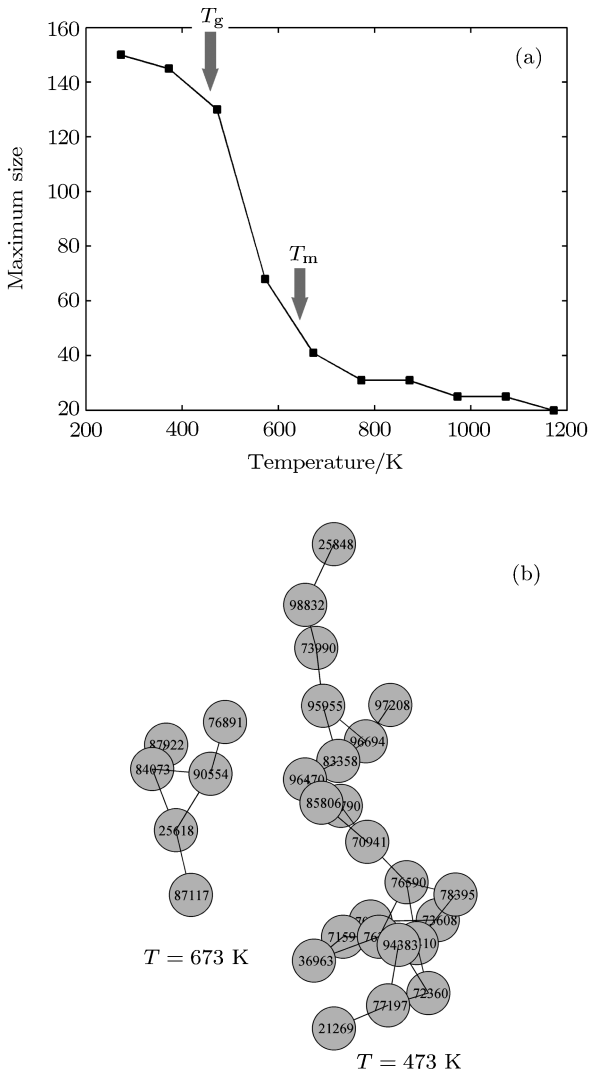


Fig. 6. Evolutions of the maximum IMRO clusters during the rapid quenching processes of $Mg_{70}Zn_{30}$ alloy. (a) Change of maximum size with temperature. (b) Schematic configurations of the combination of IS cluster bond-types in the maximum IMRO clusters at 763 K and 473 K.

maximum IMRO clusters at 763 K and 473 K, as shown in Fig. 6(b), it can be clearly seen that the icosahedral clusters have a tendency to grow in a low-dimensional way. Just in this way, the icosahedral clusters may grow indefinitely without producing a larger frustration. Since an icosahedral arrangement of thirteen Lennard–Jones atoms has a binding energy that is larger by 8.4% than an fcc or hcp arrangement,[30] and it has been demonstrated experimentally that the local icosahedral order plays a critical role in stabilizing the undercooled liquid.[31] The rapid growth of the IMRO clusters in the $Mg_{70}Zn_{30}$ alloy may stabilize its undercooled liquid and prevent crystallization, namely increase the glass formation ability.

Figure 7 further shows the size distributions of IMRO clusters in the $Mg_{70}Zn_{30}$ metallic glass at 273 K. It can be found that the IMRO clusters of certain sizes appear with higher frequency and these cluster sizes match the magic number points usually used in the research of cluster configurations when we compare their numbers with the concepts of abundance. The magic numbers 19, 23, 25, 27, 29, 31, 33, 35, 37, 39,..., are obvious, but those for larger size clusters are not clear. This magic number sequence is different from that obtained by the gaseous deposition and ionic spray methods and so on. The magic number sequence obtained from the mass spectra of Ar clusters formed in ionic spray by Harris *et al.*[32] is 13, 19, 23, 26, 29, 32, 34, 43,.... But it agrees well with the calculation results of Doye *et al.*[32] by using the potential that behaves as the glass former bulk, whose magic number sequence is 13, 19, (23), 25, (29), 31, (33), (35), 37, (39), (41), 43,... (those in brackets have actually been presented in Fig. 2(a) of Ref. [33], but have not been pointed out). Through the detailed analysis on the structures of the magic clusters in our simulations, we find that the combinations of IS bonds in them are in the form of chains or dendrites and each magic number point corresponds to one certain combining form of IS bond, as shown in Fig. 8. If we characterize the compactness of these magic clusters by the relations between the number n of icosahedra and the number Z of IS bonds in them, they can be classified into three types: the clusters with the magic number sequence 19, 25, 31, 37,..., have the least compactness, for which $Z = n - 1$ and the combinations of IS bonds display chains; the clusters with the magic number sequence 23, 29, 35,..., have the larger compactness, for which $Z = n$ and the combinations of IS bonds display dendrites; the clusters with the magic number sequence 27, 33, 39,..., have the largest compactness, for which $Z = n+1$ and the combinations of IS bonds display dendrites. These structural features of magic clusters in the $Mg_{70}Zn_{30}$ metallic glass are similar to those obtained by Doye *et al.*,[32] in which the Dzugutov magic clusters are also structured with the incompact arrangement of linked icosahedra in the form of chains or rings. However, they are remarkably different from that in Ar magic clusters formed in ionic spray, which has been proved to be compact arrangements of linked icosahedra in the closed or filling form of various parts of the icosahedral shells.[34] These differences in cluster structures may be the origin of the differences in their magic number sequences. The above analyses indicate that the IMRO in $Mg_{70}Zn_{30}$ metallic glass is characterized by certain types of extended icosahedral clusters combined by IS atoms in the form of chains or dendrites, which is different from the fcc or icosahedral building schemes for the MRO in metallic glasses proposed by Miracle[14] and Sheng,[15] respectively.

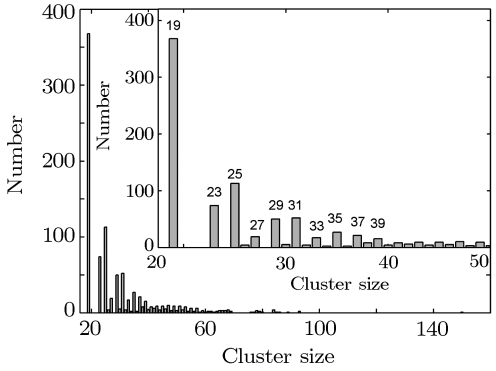


Fig. 7. Size distributions of IMRO clusters in $Mg_{70}Zn_{30}$ metallic glass (273 K).

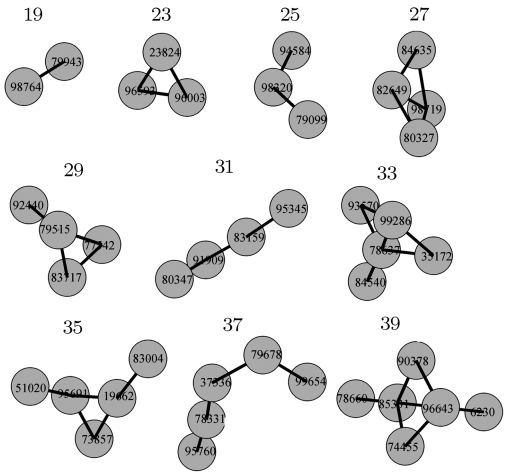


Fig. 8. Schematic configurations of the combination of IS cluster bond-types in the magic clusters.

4. Conclusions

For understanding the IMRO formed in the $Mg_{70}Zn_{30}$ metallic glass, a larger-scale system consisting of 100000 atoms has been simulated by using the MD method. The formation and structure of the IMRO in the $Mg_{70}Zn_{30}$ simple metallic glass have been investigated by means of the structural analysis methods of the PDF, HA bond-type index method and CTIM.

It is found that the simulated PDF of $Mg_{70}Zn_{30}$ metallic glass is in good agreement with the experimental results. The T_g is estimated to be 450 K under the present solidification conditions. Our calculations are very accurate in simulating the liquid quenching processes of $Mg_{70}Zn_{30}$ alloy.

The SRO in the $Mg_{70}Zn_{30}$ metallic glass is characterized by various types of basic clusters and the icosahedron is the dominant SRO structural units. The IMRO in $Mg_{70}Zn_{30}$ metallic glass is characterized by certain types of extended icosahedral clusters combined by IS atoms in the form of chains or dendrites. The size distributions of these IMRO clusters present a magic number sequence of 19, 23, 25, 27, 29, 31, 33, 35, 37, 39,. . . , and the magic clusters can be classified into three types according to their compactness. The IMRO clusters grow rapidly in a low-dimensional way with cooling, but this growth is limited near the T_g. The rapid growth of IMRO cluster in the $Mg_{70}Zn_{30}$ alloy may stabilize its undercooled liquid and prevent crystallization.

References

[1] Bian X F, Pan X M, Qin X B and Jiang M H 2002 *Sci. Chin.* Ser. E **45** 113

[2] Hou Z Y, Liu L X, Liu R S and Tian Z A 2009 *Acta Phys. Sin.* **58** 4817 (in Chinese)

[3] Hafner J 1980 *Phys. Rev.* B **21** 406

[4] Inoue A 2000 *Acta Mater.* **48** 279

[5] Andonov P and Chieux P 1987 *J. Non-cryst. Solids* **93** 331

[6] Paul F, Press W and Rabe P 1991 *J. Non-cryst. Solids* **130** 98

[7] Sadoc A, Krishnan R and Rougier P 1985 *J. Phys.* F: *Met. Phys.* **15** 241

[8] Wang R H, Ye Y F, Ming G H and Teng X Y 2007 *Acta Phys. Sin.* **50** 523 (in Chinese)

[9] Saxena N S, Bhandari D, Pratap A and Saksena M P 1990 *J. Phys.: Condens. Matter.* **2** 9475

[10] Jha N and Mishra A K 2001 *J. Alloys Compd.* **329** 224

[11] Wang S Y, Wang C Z, Li M Z, Huang L, Ott R T, Kramer M J, Sordelet D J and Ho K M 2008 *Phys. Rev.* B **78** 184204

[12] Xi X K, Li L L, Zhang B, Wang W H and Wu Y 2007 *Phys. Rev. Lett.* **99** 095501

[13] Egami T 2007 *J. Non-cryst. Solids* **353** 3666

[14] Miracle D B 2004 *Nature Mater.* **3** 697

[15] Sheng H W, Luo W K, Alamgir F M, Bai J M and Ma E 2006 *Nature* **439** 419

[16] Honeycut J D and Andersen H C 1987 *J. Phys. Chem.* **91** 4950

[17] Dong K J, Liu R S, Yu A B, Zou R P and Li J Y 2003 *J. Phys.: Condens. Matter* **15** 743

[18] Hou Z Y, Liu R S, Zheng C X, Liu H R, Tian Z A, Wang X, Zhou Q Y and Chen Z H 2007 *J. Chem. Phys.* **127** 174503

[19] Liu H R, Liu R S, Zhang A L, Hou Z Y, Wang X and Tian Z A 2007 *Chin. Phys.* **16** 3747

[20] Wang S and Lai S K 1980 *J. Phys.* F: *Met. Phys.* **10** 2717

[21] Li D H, Li X R and Wang S 1986 *J. Phys.* F: *Met. Phys.* **16** 309

[22] Wang S, Lai S K and So C B 1980 *J. Phys.* F: *Met. Phys.* **10** 445

[23] Jin Z H, Lu K, Gong Y D and Hu Z Q 1997 *J. Chem. Phys.* **106** 8830

[24] Hoover W G, Ladd A J C and Moran B 1982 *Phys. Rev. Lett.* **48** 1818

[25] Evans D J 1983 *J. Chem. Phys.* **78** 3297

[26] Wendt H R and Abraham F F 1978 *Phys. Rev. Lett.* **41** 1244

[27] Calka A 1986 *J. Phys.* F: *Met. Phys.* **16** 1577

[28] Bernal J D 1960 *Nature* **185** 68

[29] Gaskell P H 1979 *J. Non-cryst. Solids* **32** 207

[30] Frank F C 1952 *Proc. R. Soc. London* A **215** 43

[31] Kelton K F, Gangopadhyay A K, Kim T H and Lee G W 2006 *J. Non-cryst. Solids* **352** 5318

[32] Harris I A, Kidwell R S and Northby J A 1984 *Phys. Rev. Lett.* **53** 2390

[33] Doye J P K, Wales D J, Zetterling F H M and Dzugutov M 2003 *J. Chem. Phys.* **118** 2792

[34] Solov'yov I A, Solov'yov A V and Greiner W 2003 *Phys. Rev. Lett.* **90** 053401